2014

NF-kappa B-to-AP-1 Switch: A Mechanism Regulating Transition From Endothelial Barrier Injury to Repair in Endotoxemic Mice

G. Liu
Northwell Health

X. B. Ye
Northwell Health

E. J. Miller
Zucker School of Medicine at Hofstra/Northwell

S. F. Liu
Zucker School of Medicine at Hofstra/Northwell

SCIENTIFIC REPORTS

OPEN

SUBJECT AREAS:
EXPERIMENTAL MODELS OF DISEASE
APOPTOSIS
SEPSIS
MECHANISMS OF DISEASE

Received
12 March 2013

Accepted
16 June 2014

Published
2 July 2014

Correspondence and requests for materials should be addressed to S.F.L. (Sliu@lij.edu)

* These authors contributed equally to this work.

NF-κB-to-AP-1 Switch: A Mechanism Regulating Transition From Endothelial Barrier Injury to Repair in Endotoxemic Mice

Gang Liu*, Xiaobing Ye*, Edmund J. Miller & Shu Fang Liu

Centers for Heart and Lung Research and Pulmonary and Critical Care Medicine, the Feinstein Institute for Medical Research, Manhasset, NY 11030, USA.

Endothelial barrier disruption is a hallmark of multiple organ injury (MOI). However, mechanisms governing the restoration of endothelial barrier function are poorly understood. Here, we uncovered an NF-κB-to-AP-1 switch that regulates the transition from barrier injury to repair following endotoxemic MOI. Endothelial NF-κB mediates barrier repair by inhibiting endothelial cell (EC) apoptosis. Blockade of endothelial NF-κB pathway activated the activator protein (AP)-1 pathway (NF-κB-to-AP-1 switch), which compensated for the anti-apoptotic and barrier-repair functions of NF-κB. The NF-κB-to-AP-1 switch occurred at 24 hours (injury to repair transition phase), but not at 48 hours (repair phase) post-LPS, and required an inflammatory signal within the endothelium. In the absence of an inflammatory signal, the NF-κB-to-AP-1 switch failed, resulting in enhanced EC apoptosis, augmented endothelial permeability, and impeded transition from barrier injury to recovery. The NF-κB-to-AP-1 switch is a protective mechanism to ensure timely transition from endothelial barrier injury to repair, accelerating barrier restoration following MOI.

Multiple organ injury (MOI) resulting from sepsis, trauma, hemorrhage and other pathological conditions is characterized by endothelial barrier disruption and increased endothelial permeability[1–6]. Inflammatory and injurious insults cause endothelial injury and disrupt endothelial barrier integrity, resulting in leakage of fluid and protein into interstitial spaces, edema formation, multiple organ inflammation, and ultimately MOI[1–6]. Repair of the injured endothelium and restoration of normal endothelial barrier function are major factors determining organ function recovery from injury. However, there has been little research into the *in vivo* mechanisms regulating the transition from barrier injury to repair and regulating endothelial barrier recovery[7–9]. Three previous reports have demonstrated that foxhead box M1 (FoxM1)-mediated transcription of genes, controlling cell proliferation and regulating inter-endothelial junctions, are important for endothelial barrier repair following LPS-induced lung injury[7–9]. Other mechanisms and pathways regulating endothelial barrier repair following MOI remain largely unexplored. There has been no study investigating mechanisms regulating the transition from endothelial barrier injury to repair phases. As a consequence, the mechanisms and pathways regulating the transition from barrier injury to repair and endothelial barrier repair following MOI are poorly understood.

Endothelial barrier injury and repair are interrelated. Severity of injury not only determines the extent of repair, but also affects the process and speed of transitioning from injury to repair. Many genes, particular those encoding signaling molecules, are multifaceted and likely to play roles in both injury and repair. To conclusively define the role of a given gene in regulating the transition from barrier injury to repair and in regulating barrier repair, it is necessary to block the gene function only at the transition phase or at the repair phase, and not to interfere with that gene function during the organ injury phase. Only in this way, can the precise action of the gene or signaling molecule be revealed, and its regulation of injury-to-repair transition, or barrier repair, be defined unambiguously. No such study has been reported.

A major hurdle to the performance of such *in vivo* studies is the lack of useful animal models. Many transgenic (TG) or knockout mice may not be useful for such studies, because the gene of interest is inactivated during embryonic development (well before the occurrence of organ injury). Studies using those mouse models cannot

tell whether the beneficial (or detrimental) effect of the gene inactivation is a result of reduced (or enhanced) barrier injury, or a result of an enhanced (or reduced) barrier repair. Furthermore, genes important for endothelial repair can be essential for endothelial development. Disruption of the expression of these genes during embryonic development can result in endothelial structural and functional defects[10,11]. It has been reported that TG mice with endothelial specific overexpression of a mutant I-κBα (I-κBαmt) had a reduced endothelial cell (EC) tight junction density and impaired endothelial barrier function[10]. Conditional deletion of I-κB kinase β gene in ECs, using the Cre/loxP recombination system, has also been shown to increase basal endothelial permeability[11]. Thus, disruption of NF-κB signaling during embryonic development impairs basal endothelial barrier function.

We have previously created and characterized TG mice with EC-restricted expression of I-κBαmt in a doxycycline (Dox) inducible manner (EC-I-κBαmt mice)[12]. Using these mice in the current study, we developed a strategy to inhibit endothelial NF-κB activity at 24 (transition phase) or 48 (active repair phase) hours after LPS challenge in a stage-specific, and cell-targeted manner. By doing so, our original goal was to define the role of endothelial NF-κB activity in regulating endothelial barrier recovery. In the course of our study, we uncovered an "NF-κB-to-AP-1 switch" mechanism. We found that intrinsic endothelial NF-κB activity promotes endothelial barrier repair by inhibiting EC apoptosis. Blockade of the endothelial NF-κB pathway led to the activation of the activator protein (AP)-1 pathway, which compensated for the anti-apoptotic and barrier-repair functions of NF-κB. The NF-κB-to-AP-1 switch occurred at the transition phase (24 hours), but not at the repair phase (48 hours). Blockade of the NF-κB-to-AP-1 switch increased EC apoptosis, augmented endothelial permeability, and impeded the transition from endothelial barrier injury to repair phases. Thus, we have uncovered a novel NF-κB-to-AP-1 switch mechanism that serves as a protective mechanism to ensure a timely transition from endothelial barrier injury to repair phases following endotoxemic MOI, accelerating the restoration of normal endothelial barrier function.

Results

Dox-induced I-κBαmt expression at, or after, the peak of organ injury inhibits NF-κB activity. To inhibit endothelial NF-κB activity at 24 or 48 hours after LPS challenge, in a temporally-controlled manner, we first wanted to verify whether Dox treatment of the TG mice at or after peak of organ injury could effectively inhibit endothelial NF-κB activity. To determine the minimum time required for the induction of I-κBαmt mRNA expression following Dox injection, we carried out qRT-PCR analysis, which showed that I-κBαmt mRNA was barely detected at 4 hours, detected at relatively high level at 6 hours, and at higher levels at 12 and 24 hours after Dox injection in the lungs (Figure 1A). This result suggests that 4–6 hours is required to induce I-κBαmt mRNA expression, which peaked around 12 hours after LPS challenge (Figure 1A). Therefore, in our subsequent studies, we injected mice with Dox at 12 (for 24 hour group) or 36 hours (for 48 hour group) after LPS injection. Taking into account the times required to translate I-κBαmt mRNA into protein and to transport the newly synthesized I-κBαmt protein into the nucleus, the 12 hour time window allowed Dox treatment to induce sufficient I-κBαmt to effectively inhibit endothelial NF-κB activity at the desired time point.

We next examined if treatment of TG mice with Dox, at the peak of organ injury, effectively inhibits NF-κB activity at an organ level. Mice were injected with LPS and then with Dox 12 hours later to inhibit NF-κB activation at 24 hours (peak of organ injury). Using p65 nuclear translocation as a marker of NF-κB activation, we performed immunofluorescent (IF) double staining of lung sections, in which cell nuclei were stained red and p65 stained green. In cells with p65 nuclear translocation, cell nuclei contain yellow dots. The number of yellow nuclei was significantly higher in the lungs of the 24 hour WT group than in TG and control lungs at the same time point (Figure 1B). These data suggest that LPS significantly increased NF-κB activity in WT lungs and that Dox-induced I-κBαmt expression inhibited NF-κB activity in TG lungs. While it is not to illustrate an EC-selective NF-κB inhibition with IF staining alone, our previous study has clearly demonstrated that Dox-induced I-κBαmt expression and NF-κB inhibition are restricted to the EC in the TG mice used here[12]. Taken together, we have confirmed that Dox-induced I-κBαmt expression, at peak of organ injury, significantly inhibits endothelial NF-κB activity in TG mice.

We further confirmed EC-targeted NF-κB inhibition in the TG mice by measuring heart and lung tissue levels of vascular adhesion molecule-1 (VCAM-1) protein, which is an NF-κB-dependent gene product and is widely used as a marker of endothelial NF-κB activation. Western blot analysis showed that the lungs and hearts of WT animals at 24 and 48 hours post-LPS had higher tissue levels of VCAM-1 than TG mice at both time points (Figures 1C to 1F), further confirming that treatment of TG mice with Dox at or after the peak of organ injury inhibits endothelial NF-κB activity.

Characterization of natural course of endothelial barrier injury and repair following endotoxemic MOI. To better understand the process of transitioning from endothelial barrier injury to repair, we characterized the natural course by measuring endothelial permeability from onset of endotoxemia to full recovery (Figures 2A and 2B). Based on the progressive increase between 0 and 24 hours and progressive decrease between 24 and 96 hours in endothelial permeability, we defined 0–24 and 24–96 hours, respectively, as barrier injury and repair phases. Endothelial permeability peaked at 24 hours, implying that endothelial injury and repair forces are balanced at this time point. We considered 24 hours as a transition phase from barrier injury to repair. To define the role of intrinsic endothelial NF-κB activity in regulating the barrier injury to repair transition and in regulating endothelial barrier repair, our subsequent studies were focused on 24 (transition phase) and 48 hours (active repair phase).

Inhibition of endothelial NF-κB activity at 24 or 48 hours has contrasting effects on endothelial permeability. We administered Dox at 12, 36 or 84 hours after LPS to inhibit endothelial NF-κB activity during transition, active repair or late repair phase separately. We then measured endothelial permeability. Endothelial NF-κB blockade at 96 hours had no effect on endothelial permeability (Figures 2C and 2D), which is consistent with endothelial barrier function having recovered (Figures 2A and 2B). Endothelial NF-κB blockade at 48 hours augmented endothelial permeability (Figures 2C and 2D), indicating that endothelial NF-κB activity is critically required for endothelial barrier repair and restoration. By contrast, endothelial NF-κB blockade at 24 hours attenuated LPS-induced endothelial permeability (Figures 2C and 2D). Thus, stage-specific blockade of endothelial NF-κB activity at 24 and 48 hours had contrasting effects on endothelial permeability.

Inhibition of endothelial NF-κB activity at 48, but not at 24, hours enhances EC apoptosis. Endothelial apoptosis is an important cause of endothelial permeability[13–17]. To explain why endothelial NF-κB blockade at 24 and 48 hours had different effects on endothelial permeability, we compared the effects of endothelial NF-κB blockade on EC apoptosis in the lungs between 24 and 48 hours post-LPS. We chose to study lungs because they are enriched in ECs. We labeled apoptotic ECs using CD31 and Tunel (terminal deoxynucleotidyl transferase dUTP nick end labeling) double staining. We verified that the CD31 antibody reacts with ECs, but does not cross-react with epithelial cells or basal membrane components (Supplementary Figures 1A and 1B), and that CD31

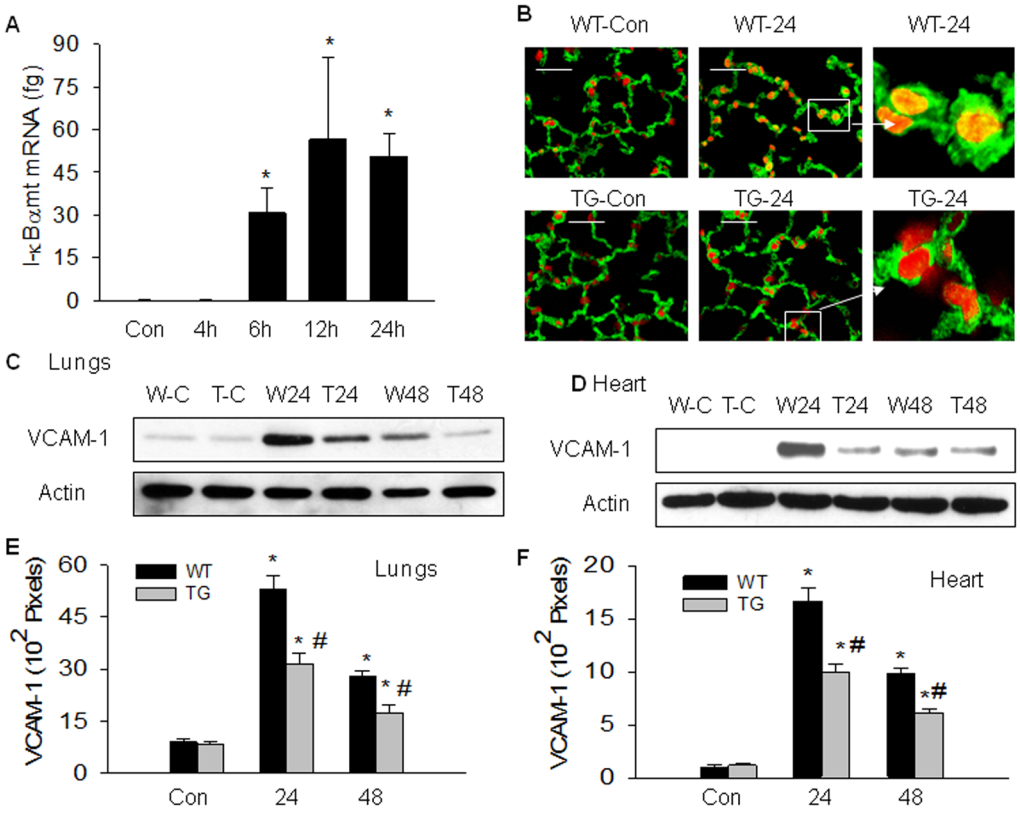

Figure 1 | Dox-induced I-κBαmt expression at or after peak of organ injury inhibits endothelial NF-κB. (A): Time course of Dox-induced I-κBαmt mRNA expression. TG mice were injected with saline or doxycycline (Dox, 0.5 mg/mouse, i.p.), and lungs harvested at 4, 6, 12 and 24 hours after Dox or 24 hours after saline (Con) injection. Tissue level of I-κBαmt mRNA was quantified by qRT-PCR, and expressed as fg I-κBαmt cDNA in 500 ng total cDNA. *, $p < 0.05$, compared to Con and 4 h groups. Mean ± SEM of 5 mice per group. (B): Dox-induced I-κBαmt expression at peak of organ injury inhibits NF-κB activity. Mice were injected with saline (Con groups) or LPS (5 mg/kg, i.p., 24 hour groups), and then with Dox (0.5 mg/mouse, i.p.) 12 hours later to inhibit endothelial NF-κB at 24 hours post-LPS, when lung cryosections were prepared. Cell nuclei were stained red using propidium iodide (IP) and p65-expresing cells stained green using fluorescent antibody. Cell nuclei become yellow in cells with p65 nuclear translocation (an indicator of NF-κB activity). LPS increased number of PI+/p65+ yellow nuclei in WT-24 lungs, but not in TG-24 lungs, indicating an inhibition of NF-κB activity in TG mice. Scale bar, 50 μm. Representative of 3 independent experiments. Arrow indicates detailed view showing that number of PI+/p65+ nuclei was significantly reduced in TG lungs. (C–F): Dox-induced I-κBαmt expression inhibits VCAM-1 expression. Mice were injected with saline or LPS, and then with Dox 12 (for 24 hour group) or 36 (for 48 hour group) hours after LPS injection to inhibit endothelial NF-κB in TG mice at 24 or 48 hours, when tissue levels of vascular cell adhesion molecule-1 (VCAM-1) were determined. (C) and (D): Western blot photographs show that LPS-induced VCAM-1 expression was inhibited in TG mice. Cropped blots are used. Full-length blots are shown in Supplementary Figure 4. (E) and (F): The VCAM-1 bands were quantified using densitometry and expressed as $\times 10^2$ pixels. *, $p < 0.05$, compared with controls. #, $p < 0.05$, compared to WT-24 or WT-48 group. Mean ± SEM of 5 mice per group.

and Tunel staining reliably labels apoptotic ECs in lungs (Supplementary Figures 1C and 1D).

LPS significantly increased the number of $Tunel^+/CD31^+$ apoptotic ECs, and the number of apoptotic ECs peaked at 24 hours and then were reduced at 48 hours after LPS administration (Figure 3). Inhibition of endothelial NF-κB activity at 24 hours had no effect on EC apoptosis. By contrast, inhibition of endothelial NF-κB activity at 48 hours markedly increased the number of apoptotic ECs (Figure 3), and the timing of this increase correlated well with the augmented endothelial permeability caused by endothelial NF-κB blockade at 48 hours (Figures 2C vs 3B). This result suggests that an increased EC apoptosis underlies the augmented endothelial permeability caused by endothelial NF-κB inhibition at 48 hours.

LPS increased both the pro-apoptotic protein, Bax, and anti-apoptotic protein, Bcl-2, expression in the lungs, which peaked at 24 and 48 hours, respectively (Supplementary Figure 2). Consistent with the effects on EC apoptosis, endothelial NF-κB blockade at 24 hours had no effect on Bax and Bcl-2 expression, but at 48 hours significantly enhanced Bax and inhibited Bcl-2 expression (Supplementary Figure 2).

Inhibition of EC apoptosis reverses the augmented endothelial permeability at 48 hours. To confirm that an enhanced EC apoptosis is the cause of the augmented endothelial permeability associated with endothelial NF-κB inhibition at 48 hours, we treated mice with a caspase inhibitor, Z-VAD-FMK, which has been widely used to inhibit cell apoptosis in various models, including sepsis[18,19]. LPS caused an increase, in WT mice (without endothelial NF-κB inhibition), and a greater increase, in TG mice (with endothelial NF-κB inhibition), in endothelial permeability (Figure 4), demonstrating an augmentation of endothelial permeability by endothelial NF-κB blockade. Z-VAD-FMK treatment reversed the augmented endothelial permeability (Figure 4), establishing a link between the enhanced EC apoptosis and augmented endothelial permeability caused by endothelial NF-κB inhibition at 48 hours.

Inhibition of endothelial NF-κB activity at 24, but not at 48, hours leads to NF-κB-to-AP-1 switch. To uncover the mechanisms underlying the different effects of endothelial NF-κB blockade on EC apoptosis between 24 and 48 hours, we analyzed lung tissue levels

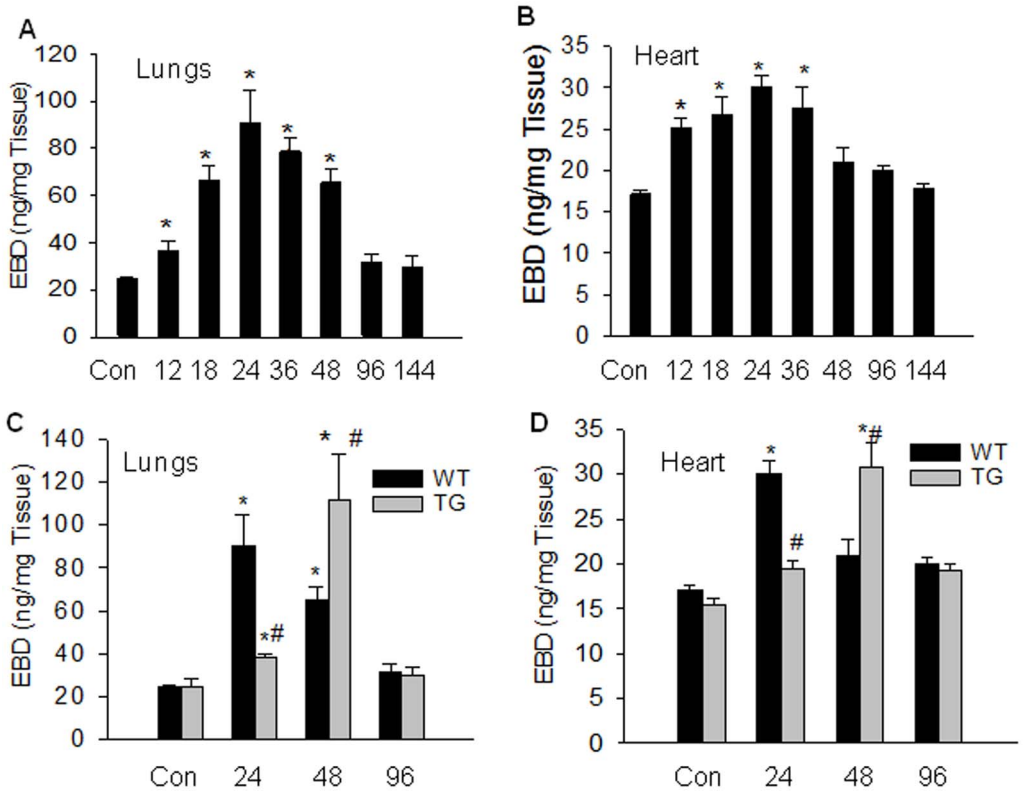

Figure 2 | Contrast effects of endothelial NF-κB inhibition at 24 and 48 hours on endothelial permeability. (A) and (B): Natural course of endothelial barrier injury and recovery: WT mice were injected with saline (Con) or LPS (5 mg/kg, i.p.), and endothelial permeability in lungs and heart measured at 12, 18, 24, 36, 48, 96 or 144 hours after LPS injection using Evan blue dye (EBD) leakage index as an indicator. Transition from barrier injury to repair phase occurs at 24 hours, and active barrier repair phase occurs at 48 hours after onset of endotoxemia. Means ± SEM of 5 mice per group. *, $p < 0.0.5$, compared to controls. (C) and (D): Contrast effects of endothelial NF-κB inhibition at 24 and 48 hours on endothelial permeability: TG mice were injected with saline (Con) or LPS and then with Dox (0.5 mg/mouse, i.p.) 12 (24 hour groups), 36 (48 hour groups) or 84 (96 hour groups) hours after LPS injection Endothelial permeability was measured at 24, 48 or 96 hours after LPS injection. Inhibition of endothelial NF-κB at 48 (active repair phase), but not at 24 (transition phase), hours augmented endothelial permeability. Means ± SEM of 6 mice per group. *, $p < 0.0.5$, compared to controls. #, $p < 0.05$, compared to respective WT-24 or WT-48 groups.

of a panel of apoptosis regulating proteins. We found that tissue levels of AP-1 family of proteins, *c-Jun* and *c-Fos*, were differentially affected by endothelial NF-κB blockade at 24 and 48 hours. Endothelial NF-κB blockade at 24 hours increased nuclear levels of *c-Jun* and *c-Fos* proteins by 2-fold, whereas endothelial NF-κB blockade at 48 hours reduced the nuclear level of *c-Jun* but had no effect on the nuclear level of *c-Fos* protein (Figures 5A–5D).

IF staining demonstrated that TG lungs 24 hour after LPS challenge had significantly higher numbers of $CD31^+/c\text{-}Jun^+$ ECs compared to TG lungs after 48 hour, or WT lungs after 24 or 48 hours (Figure 5E). Thus, blockade of the endothelial NF-κB pathways led to the activation of AP-1 pathway (NF-κB-to-AP-1 switch), which occurred at 24 (transition phase), but not at 48 hours (repair phase).

Blockade of the NF-κB-to-AP-1 switch mechanism at 24 hours promotes EC apoptosis. To understand the biological function of the NF-κB-to-AP-1 switch, we inhibited the compensatory AP-1 activity induced by endothelial NF-κB blockade at 24 hours, and examined the effect of this inhibition on EC apoptosis. We inhibited AP-1 activity by overexpressing a dominant negative *c-Jun*, TAM67, which specifically inhibits AP-1 activity[20,21], and by pretreating mice with SP60012, which selectively inhibits JNK activity[22].

Previous reports show that intravenous administration of DNA-liposome complexes resulted in transgene expression predominantly in the lungs, particularly in lung ECs[23]. We took advantage of this gene transfer approach to deliver the TAM67 transgene into lung ECs. IF staining showed that lung sections from mice transfected with pCMV-TAM67 displayed a many fold increase in numbers of $CD31^+/c\text{-}Jun^+$ ECs, compared to lung sections from mice transfected with the pCMV-vector alone (Supplementary Figure 3). This result confirms that TAM67 was overexpressed predominantly in lung ECs.

Tunel and CD31double staining showed that LPS significantly increased the number of $Tunel^+/CD31^+$ apoptotic ECs in lungs (Figure 6). Inhibition of the compensatory AP-1 activity by TAM67 overexpression or by SP600125 treatment augmented LPS-induced increase in the number of apoptotic ECs in the presence (TG lungs), but not in the absence (WT lungs), of endothelial NF-κB blockade (Figure 6). Thus, blockade of the NF-κB-to-AP-1 switch at 24 hours augmented EC apoptosis, which mimics the effect of endothelial NF-κB blockade at 48 hours. This result indicates that activation of the NF-κB-to-AP-1 switch mechanism is responsible for the lack of effect of endothelial NF-κB inhibition on EC apoptosis at 24 hours. Differential activation of the switch mechanism explains the contrasting effects of endothelial NF-κB blockade on EC apoptosis between 24 and 48 hours.

Blockade of NF-κB-to-AP-1 switch mechanism at 24 hours augments endothelial permeability. To better understand the physiological function of the switch mechanism, we blocked the NF-κB-to-AP-1 switch by TAM67 overexpression, which inhibited the compensatory AP-1 activity and thereby the switch mechanism. We then examined the effect of this blockade on endothelial

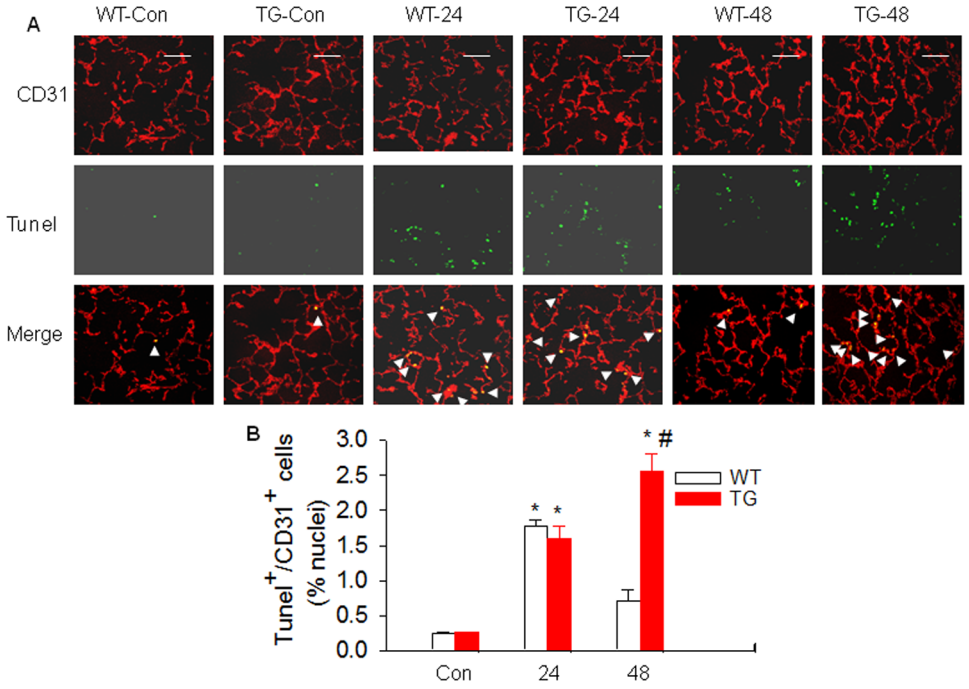

Figure 3 | Endothelial NF-κB inhibition at 48, but not 24, hours enhances EC apoptosis. Mice were injected with saline or LPS as described above, and then with Dox 12 (24 hour groups) or 36 hours (48 hour groups) after LPS injection. Lung cryosections were prepared at 24 or 48 hours after LPS injection and double stained with Tunel reaction mixture and CD31 antibody to identify apoptotic endothelial cells (ECs). (A): Representative micrographs of CD31 (red) and Tunel (green) double staining of lung section. Endothelial NF-κB inhibition at 48 hours significantly increased, but at 24 hours had no effect on the number of Tunel+/CD31+ apoptotic ECs (arrowhead indicated). Scale bar, 50 μm. (B): Bar graphic representation of apoptotic ECs. Number of Tunel+/CD31+ cells in each lung cryosection was counted and expressed as a percentage of total cell nuclei. Mean ± SEM of 5 mice per group. *, $p < 0.05$, compared with control groups. #, $p < 0.05$, compared to WT-48 group.

permeability. LPS significantly increased lung endothelial permeability in both WT and TG mice (Figure 7). TAM67 overexpression in WT mice at 24 hours (no NF-κB inhibition and no NF-κB-to-AP-1 switch) had no effect on LPS-induced endothelial permeability. However, in TG mice at 24 hours (with NF-κB inhibition and NF-κB-to-AP-1 switch), there was an augmentation in the LPS-induced endothelial permeability (Figure 7A). TAM67 overexpression in TG mice at 48 hours (with NF-κB inhibition, but no NF-κB-to-AP-1 switch) had no effect on endothelial permeability induced by LPS plus NF-κB inhibition (Figure 7B). This result shows that blockade of the NF-κB-to-AP-1 switch mechanism augmented LPS-induced endothelial permeability, suggesting a barrier-protective function for the switch mechanism.

An inflammatory signal is necessary for the NF-κB-to-AP-1 switch. In searching for an answer to why NF-κB-to-AP-1 switch

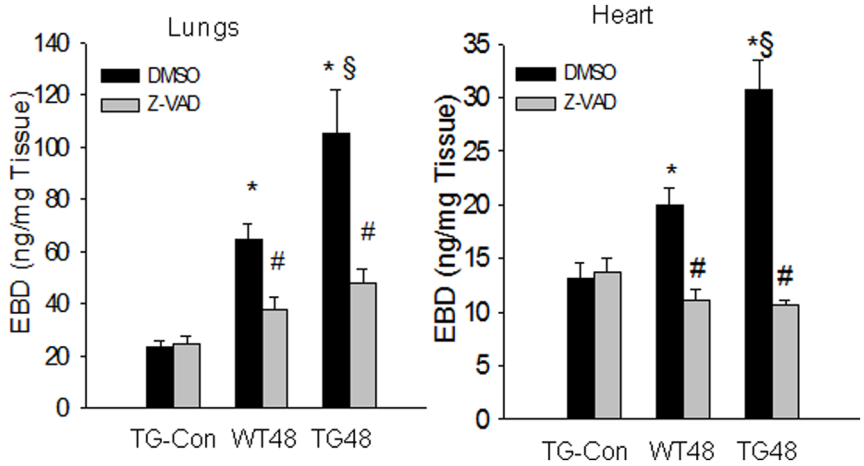

Figure 4 | Inhibition of cell apoptosis reverses the augmented endothelial permeability caused by endothelial NF-κB inhibition at 48 hours. Mice were injected with saline or LPS and simultaneously with the caspase inhibitor, Z-VAD-FMK (Z-VAD, 3 mg/kg, i.v.) or DMSO, solvent of Z-VAD-FMK. Additional dose of Z-VAD-FMK was given (i.p.) every 12 hours. All mice were injected with Dox 36 hours after LPS or saline injection. Endothelial permeability in lungs and heart was measured 48 hours after LPS injection using EBD leakage index as an indicator. Means ± SEM of 6 mice per group. *, $p < 0.05$, compared with TG-con groups. #, $p < 0.05$, compared with respective DMSO treated groups. §, $p < 0.05$, compared with WT48 DMSO treated group. DMSO and Z-VAD had no effect on endothelial permeability in WT-con mice.

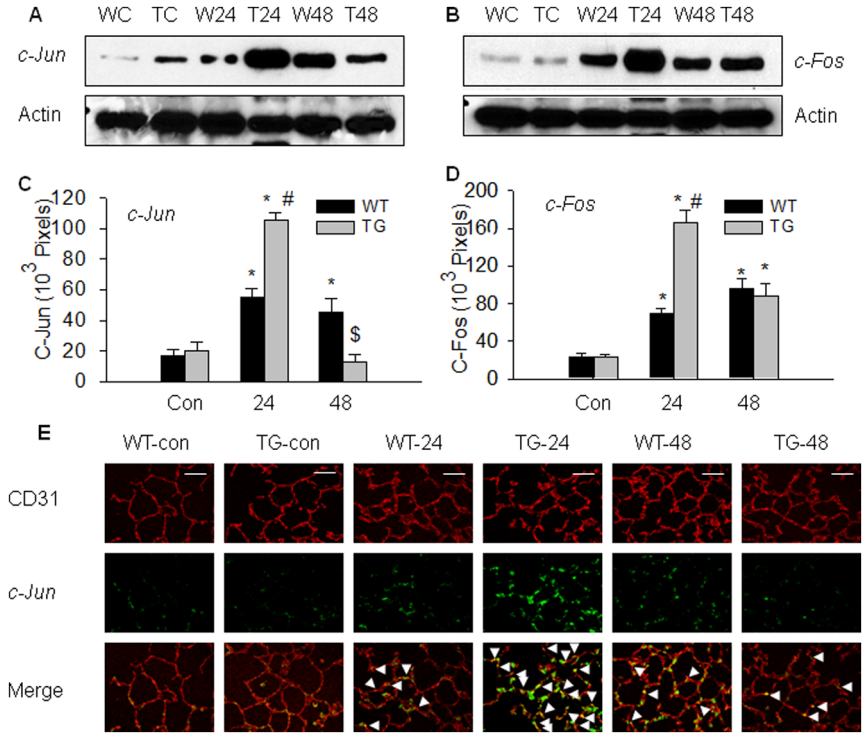

Figure 5 | Blockade of endothelial NF-κB pathway at 24, but not at 48, hours activates AP-1 pathway. Mice were injected with saline, LPS and Dox as described above. Nuclear levels of *c-Jun* and c-*Fos* proteins in lungs of control (WC and TC), 24 (W24 and T24) and 48 (W48 and T48) hour groups of WT and TG mice were determined by Western blot. (A) and (B): Western blot photographs show that inhibition of endothelial NF-κB at 24, but not at 48, hours increased nuclear levels of *c-Jun* and c-*Fos* in TG lungs. Cropped blots are used. Full-length blots are shown in Supplementary Figure 4. (C) and (D): The *c-Jun* and c-*Fos* protein bands were quantified using densitometry and expressed as $\times 10^3$ pixels. Means ± SEM of 6 mice each group. *, $p < 0.05$, compared with WC and TC groups. #, $p < 0.05$, compared with WT-24, WT-48 or TG-48 group. $, $p < 0.05$, compared with WT-48 group. (E). Representative micrographs of CD31 (red) and *c-Jun* (green) double stains of lung sections show that endothelial NF-κB inhibition at 24 (WT-24 vs TG-24), but not at 48 (WT-48 vs TG-48), hours significantly increased *c-Jun*+/CD31+ cells (arrow indicated) in lungs. Scale bar, 50 μm.

occurred at 24, but not at 48 hours, we noted that tissue level of VCAM-1 was significantly higher at 24 hours than at 48 hours (Figures 1C to 1F), suggesting that a level of inflammation within endothelium is necessary for the NF-κB-to-AP-1 switch to occur. To test this possibility, we stimulated cultured ECs from TG mouse lungs with a threshold concentration of LPS or Dox (to inhibit endothelial NF-κB), or a combination of the two, and measured the nuclear level of *c-Jun*. LPS or Dox alone caused an increase, but LPS+Dox caused a greater increase in nuclear level of *c-Jun* (Figure 8A). Thus, an inflammatory signal in the endothelium is necessary for the NF-κB-to-AP-1 switch to occur.

Endothelial NF-κB blockade increases AP-1 activity. Since AP-1 activity is critically regulated by *c-Jun* phosphorylation at Ser63 and Ser73[24,25], we determined the nuclear level of phospho-*c-Jun* (Ser63). Dox or LPS alone had no effect on *c-Jun* phosphorylation, but Dox+LPS markedly increased the nuclear level of phospho-*c-Jun* (Figure 8B). Consistent with *c-Jun* phosphorylation, stimulation of TG ECs with Dox or LPS alone induced an increased *c-Jun* binding activity. However, there was a significantly greater increase in *c-Jun* binding activity when cells were treated with a combination of Dox and LPS (Figure 8C). Thus, endothelial NF-κB blockade stimulates AP-1 binding activity in the presence of an inflammatory signal.

JNK activation is involved in the NF-κB-to-AP-1 switch. *C-Jun* phosphorylation at Ser63 and Ser73 is primarily mediated by *c-Jun* NH_2-terminal kinases (JNKs)[26]. JNK is activated by dual phosphorylation of threonine and tyrosine residues (Thr183/Tyr185) within the Thr-Pro-Tyr motif[27]. We found that tissue level of phospho-JNK (an indicator of JNK activation) was significantly higher in the TG lungs after 24 hours than at 48 hours. The phospho-JNK in TG lungs was also higher than in the lungs of WT mice, (Figure 8D). Inhibition of JNK activity, achieved by pretreating mice with a selective JNK inhibitor SP600125[22], reduced the tissue level of phospho-*c-Jun* in TG lungs at 24 hours (Figure 8E), suggesting that JNK activation is involved in the process that leads to the NF-κB-to-AP-1 switch.

Discussion

This study uncovers a novel NF-κB-to-AP-1 switch mechanism that regulates the transition from endothelial barrier injury to repair *in vivo*. Inhibition of endothelial NF-κB activity, at 24 hours after LPS challenge, induced a significant AP-1 activity (NF-κB-to-AP-1 switch), in the absence of any change in EC apoptosis. By contrast, inhibition of endothelial NF-κB activity at 48 hours post-LPS failed to induce AP-1 activity (no NF-κB-to-AP-1 switch) and resulted in an enhanced EC apoptosis and augmented endothelial permeability. Differential activation of the switch mechanism underlies the contrasting effects of endothelial NF-κB blockade on EC apoptosis between 24 and 48 hours post-LPS. Inhibition of the NF-κB-to-AP-1 switch at 24 hours enhanced EC apoptosis and augmented endothelial permeability, which mimicked the effect of endothelial NF-κB blockade at 48 hours. Thus, blockade of endothelial NF-κB pathways at 24 hours led to activation of AP-1 pathway (NF-κB-to-AP-1 switch), which compensated for the anti-apoptotic and barrier-protective functions of NF-κB, preventing the increase in EC apoptosis and the augmentation of endothelial permeability. Failure to activate the switch mechanism led to an enhanced EC apoptosis and augmented endothelial permeability following endothelial NF-κB inhibition. Since the NF-κB-to-AP-1 switch occurs at the transition, but not at the repair phase, this mechanism

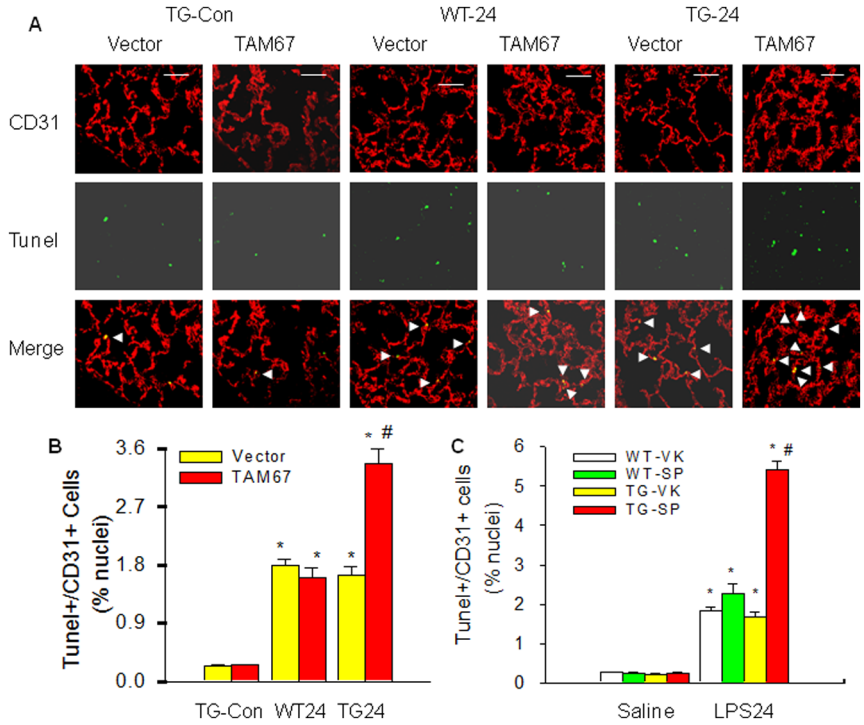

Figure 6 | Blockade of NF-κB-to-AP-1 switch at 24 hours enhances EC apoptosis. Mice in the vector and TAM67 groups were transfected with pCMV-vector or pCMV-TAM67 cDNA encoding a dominant negative *c-Jun*. Mice in WT-VK and TG-VK groups were injected with PPCES vehicle and in WT-SP and TG-SP groups were injected with SP600125. Fifteen minutes after SP600125 injection, or 3 days after DNA transfection, mice were injected with saline or LPS as described above, and then with Dox 12 hours after LPS injection. Lung cryosections were prepared 24 hours after LPS injection and double stained with Tunel reaction mixture and CD31 antibody. (A): Representative micrographs of CD31 (red) and Tunel (green) double stainings show that TAM67 overexpression (inhibiting NF-κB-to-AP-1 switch mechanism) augmented LPS-induced EC apoptosis in TG lungs (TG-24, arrowhead indicated). Scale bar, 50 μm. (B): Bar graph shows that inhibition of NF-κB-to-AP-1 switch by TAM67 overexpression at 24 hours enhanced EC apoptosis in TG lungs. The number of Tunel+/CD31+ apoptotic ECs in each lung cryosection was counted and expressed as a percentage of total nuclei. Means ± SEM of 5 mice per group. *, $p < 0.05$, compared with vector and TAM67 control groups. #, $p < 0.05$, compared with WT-24 vector, WT-24 TAM67 and TG-24 vector group. (C): Bar graph shows that inhibition of NF-κB-to-AP-1 switch using JNK inhibitor, SP600125, enhanced EC apoptosis in TG lungs. Number of Tunel+/CD31+ apoptotic ECs in each lung cryosection was counted and expressed as a percentage of total nuclei. Mean ± SEM of 5 mice per group. *, $p < 0.05$, compared with saline control groups. #, $p < 0.05$, compared with other LPS 24 groups.

is unlikely to play a direct role in regulating endothelial barrier recovery. However, this switch mechanism could play an important role in accelerating the transition from barrier injury to repair phase, which does promote endothelial barrier recovery.

Several lines of evidence suggest that enhanced EC apoptosis is responsible for the augmented endothelial permeability caused by endothelial NFκB blockade at 48 hours. First, LPS-induced EC apoptosis is temporally correlated with LPS-induced increase in endothe-

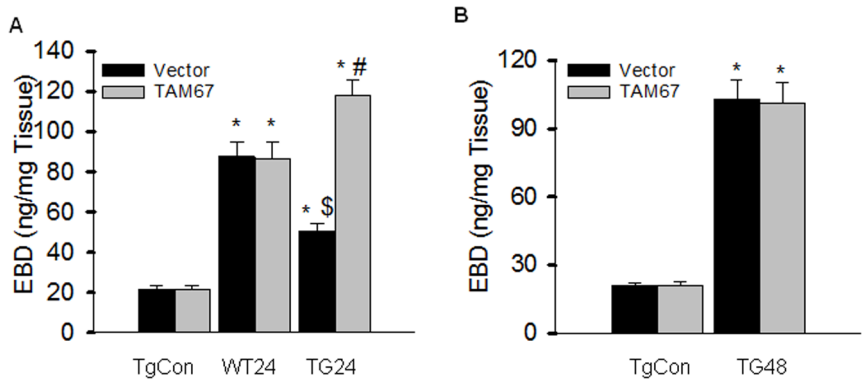

Figure 7 | Blockade of the NF-κB-to-AP-1 switch augments endothelial permeability. Mice were transfected with pCMV-vector or pCMV-TAM67 plasmid. At 3 days after transfection, mice were injected with saline or LPS, and then with Dox 12 (for 24 hours) or 36 (for 48 hours) hours after LPS injection. Endothelial permeability was measured at 24 or 48 hours after LPS injection. (A). TAM67 overexpression at 24 hours (inhibiting the NF-κB-to-AP-1 switch) augmented endothelial permeability in the presence (TG24), but not in the absence (WT24), of endothelial NF-κB blockade. (B). TAM67 overexpression at 48 hours in TG mice (with endothelial NF-κB blockade, but no NF-κB-to-AP-1 switch) had no effect on endothelial permeability. Means ± SEM of 7 (A) or 5 (B) mice per group. *, $p < 0.05$, compared with TG-con groups. #, $p < 0.05$, compared with WT24 vector, WT24 TAM67 or TG24 vector group. $, $p < 0.05$, compared with WT24 vector group.

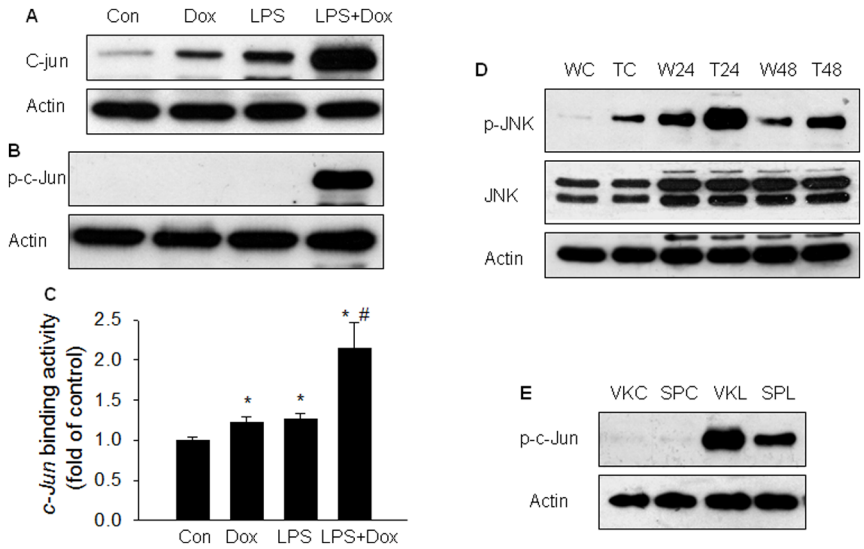

Figure 8 | Mechanism of NF-κB-to-AP-1 switch. (A–C): Blockade of the NF-κB pathway activates AP-1 pathway in the presence of an inflammatory signal. Microvascular ECs from TG lungs were unstimulated (Con), or stimulated with LPS (0.1 ng/ml) or Dox (100 μg/ml) alone or LPS + Dox. At 24 hours after stimulation, the nuclear level of *c-Jun* or phospho-*c-Jun* (Ser63) protein was determined or *c-Jun* DNA binding activity measured. Cropped blots are used for Western blot photographs. Full-length blots are shown in Supplementary Figure 4. (A): Western blot photographs show that LPS or Dox stimulation alone caused an increase, but LPS + Dox stimulation caused a greater increase in nuclear *c-Jun* level. Representative of 3 independent experiments. (B): Western blot photographs show that LPS or Dox stimulation alone did not, but LPS + Dox stimulation increased nuclear phospho-*c-Jun* (*p-c-Jun*, Ser63) level. Representative of 3 independent experiments. (C): Bar graph shows that LPS or Dox stimulation alone caused an increase, and LPS + Dox stimulation caused a greater increase in *c-Jun* DNA binding activity. Data was presented as fold change over control. Means ± SEM of 6 independent observations. *, $p < 0.05$, compared to control. #, $p < 0.05$, compared to other 3 groups. (D) and (E): JNK activity is involved in NF-κB-to-AP-1 switch. (D): Western blot photographs show that endothelial NF-κB inhibition at 24 hours increased JNK activity. Mice were injected with saline, LPS and Dox as described above. Tissue levels of total *c-Jun* N-terminal kinase (JNK) protein and phospho-JNK (p-JNK, Thr183/Tyr185, an indicator of JNK activity) in lungs of control (WC and TC), 24 (W24 and T24) and 48 (W48 and T48) hour groups of WT and TG mice were determined. Representative of 3 independent experiments. (E): JNK inhibitor reduced *c-Jun* phosphorylation. Mice were pretreated with JNK inhibitor, SP600125, and injected with saline, LPS and Dox as described above. Nuclear level of phospho-*c-Jun* (*p-c-Jun*) in lungs from vehicle control (VKC), SP600125 control (SPC), vehicle LPS (VKL) and SP600125 LPS (SPL) groups of TG mice were determined by Western blot. The data shown is representative of 3 independent experiments.

lial permeability. Although the numbers of apoptotic ECs are only a small fraction of the total ECs, EC apoptosis leads to the formation of pores in the endothelial layer, which dramatically increase endothelial leakiness. Second, endothelial NFκB inhibition at 48 hours post-LPS concomitantly increased EC apoptosis and endothelial permeability. Third, a causal link between EC apoptosis and increased endothelial permeability has been demonstrated previously[15–17]. Fourth, inhibition of EC apoptosis prevented the augmentation of endothelial permeability caused by endothelial NFκB blockade. Fifth, blockade of the NF-κB-to-AP-1 switch at 24 hours enhanced EC apoptosis and concurrently augmented endothelial permeability.

In addition to regulating cell apoptosis and proliferation, NF-κB mediates inflammatory gene expression[6] and causes myosin light chain phosphorylation, actin filament reorganization, and cytosolic translocation of junction proteins[28–31], resulting in disruption of endothelial tight/adherens junctions. However, these mechanisms are unlikely to contribute to the augmented endothelial permeability caused by endothelial NFκB blockade at 48 hours. These molecular and biochemical events are early events and have been reversed at 48 hours after LPS challenge[8,12,28–31]. Furthermore, inhibition of NF-κB-mediated inflammatory gene expression and reversal of NF-κB-mediated endothelial tight/adherens junction disruption by NF-κB blockade decrease, but not increase, endothelial permeability[28–31]. Collectively, we have demonstrated an NF-κB-to-AP-1 switch mechanism that serves as a protective mechanism against EC apoptosis and permeability increase, when endothelial NF-κB pathway is blocked.

The NF-κB-to-AP-1 switch appears to be exquisitely fine-tuned. The numbers of apoptotic ECs were comparable between TG and WT lungs at 24 hours, although the NF-κB-to-AP-1 switch occurred in TG, but not in WT lungs. The extent of EC apoptosis is determined by the balance between pro- and anti-apoptotic factors. The equal numbers of apoptotic ECs in WT and TG lungs suggest that the NF-κB-mediated (in WT mice) and the AP-1-mediated (in TG mice) anti-apoptotic activities were equivalent, assuming that the pro-apoptotic forces were matched, as should be, between WT and TG lungs and that anti-apoptotic factors other than NF-κB or AP-1 were not affected by endothelial NF-κB blockade. This means that endothelial NF-κB blockade in TG lungs stimulated an AP-1 activity that just compensated for the lost NF-κB activity. As a result, the numbers of apoptotic ECs in WT and TG mice at 24 hours were similar. This interpretation also explains why TAM67 overexpression at 24 hours augmented EC apoptosis in TG, but not in WT mice. The NF-κB-to-AP-1 switch occurred in TG, but not in WT mice. TAM67 overexpression inhibited AP-1-mediated anti-apoptotic activity in TG, but had no effect on NF-κB-mediated anti-apoptotic activity in WT mice. Consequently, TG mice overexpressing TAM67 had increased apoptotic ECs.

Our observation that TAM67 overexpression augmented LPS-induced EC apoptosis in TG, but not in WT mice, indicates that the AP-1-mediated anti-apoptotic mechanism is activated only when NF-κB-mediated anti-apoptotic signal is blocked. This is highly concordant with the notion that the NF-κB-to-AP-1 switch is a compensatory mechanism. Although this mechanism may not operate in WT mice, its significance cannot be diminished under pathological conditions when endothelial NF-κB signaling is disrupted. Since the switch occurs at the transition phase from endothelial barrier injury to repair, the NF-κB-to-AP-1 switch may serve as a backup protect-

ive mechanism to ensure a timely transition from barrier injury to repair phases following endotoxemic MOI. Our demonstration that blocking the NF-κB-to-AP-1 switch by TAM67 overexpression at 24 hours augmented endothelial permeability supports this view.

Nuclear levels of *c-Jun* and *c-Fos* proteins were higher in LPS-challenged lungs than in control lungs at 24 and 48 hours in both WT and TG nice, suggesting that there remains LPS-induced AP-1 activity at 24 and 48 hours after challenge. However, this AP-1 activity does not appear to contribute to the anti-apoptotic and barrier-protective actions of the NF-κB-to-AP-1 switch mechanism. Nor does it regulate the transition from barrier injury to repair. Inhibition of this AP-1 activity by TAM67 overexpression at 24 hours had no effects on EC apoptosis and endothelial permeability in WT mice. The potential role of the LPS-induced AP-1 activity in endothelial barrier repair warrants further investigation.

We observed that an inflammatory signal is required for NF-κB-to-AP-1 switch to occur. Since the switch mechanism regulates the transition from barrier injury to repair, this result implies a beneficial effect of a level of inflammation in the transition from barrier injury to repair. Our result is consistent with a recent report showing that inflammation activates regenerative programs in the brains of zebra fish[32]

JNK activity plays a role in the NF-κB-to-AP-1 switch. Endothelial NF-κB inhibition activated JNK at 24 hours, when the NF-κB-to-AP-1 switch occurred, but not at 48 hours, when NF-κB-to-AP-1 switch did not occur. Treatment of TG mice with a selective JNK inhibitor reduced *c-Jun* phosphorylation evoked by endothelial NF-κB blockade, and diminished the anti-apoptotic actions of the NF-κB-to-AP-1 switch. A negative crosstalk between NF-κB and JNK-AP-1 pathways has been previously reported in cultured tumor cells[33–35]. NF-κB activation induces X-chromosome-linked inhibitor of apoptosis, and growth arrest and DNA damage 45β[33,35], which directly binds to MKK7/JNKK2, the activator of JNK, and blocks its catalytic activity, leading to a suppression of JNK activation[35]. Although this mechanism has not been demonstrated in ECs, it is possible that endothelial NF-κB blockade disrupts the crosstalk and relieves the inhibition, leading to JNK activation and subsequent activation of AP-1 pathways.

Endothelial NF-κB inhibition at 24 and 48 hours after LPS challenge exerted contrasting effects on endothelial permeability, increasing permeability at 48 hours (repair phase), but decreasing permeability at 24 hours (transition phase). The opposite effects of NF-κB inhibition are mediated by different mechanisms. NF-κB plays dual roles in LPS-induced endothelial permeability. NF-κB mediates LPS-induced increase in endothelial permeability by disrupting inter-endothelial junctions (paracellular mechanisms), as results of inflammatory gene expression, myosin light chain phosphorylation, endothelial cytoskeletal reorganization and junction protein cytosolic translocation[6,8,28–31]. NF-κB inhibits LPS-induced endothelial permeability by suppressing EC apoptosis (apoptotic mechanism). The net effect of NF-κB inhibition on endothelial permeability depends on which of the underlying mechanisms is predominantly affected. At 48 hours, LPS-triggered inflammatory response has been greatly dampened, the disrupted inter-endothelial junctions have been restored, resulting in EC apoptosis as the predominant mechanism underlying the increased endothelial permeability. Endothelial NF-κB inhibition at this stage augmented endothelial permeability by promoting EC apoptosis, without significantly involving the paracellular mechanisms. At 24 hours, LPS-induced organ inflammation remains, inter-endothelial junction disruption persists and EC apoptosis peaks. Endothelial NF-κB inhibition at 24 hours inhibited both paracellular and apoptotic mechanisms. However, endothelial NF-κB inhibition activates the NF-κB-to-AP-1 switch mechanism, which compensates for the anti-apoptotic function of NF-κB, resulting in no change in EC apoptosis. Consequently, endothelial NF-κB inhibition at 24 hours reduced endothelial permeability by mitigating LPS-induced endothelial inflammation and disruption of inter-endothelial junctions, without involving the apoptotic mechanism. In supporting this explanation, we demonstrated here that tissue level of VCAM-1 is remarkably higher at 24 than at 48 hours in lungs and heart, and that inhibition of endothelial NF-κB at 48 hours, but not 24 hours, enhances EC apoptosis. This explanation is consistent with our observation that 24 hours is at the peak of the barrier injury phase, while 48 hours is at the active barrier repair phase.

Although the role of NF-κB in endothelial barrier injury has been extensively studied[6,12,36], this is the first study demonstrating that NF-κB plays a role in endothelial barrier repair and restoration. NF-κB is a multi-faceted transcription factor involved in multiple cellular and pathological processes[6,36–41]. It is not surprising that endothelial NF-κB plays such a role. Importantly, there are a variety of mechanisms that determine the many different effects of activating the same NF-κB pathway. In this context, our demonstration that endothelial NF-κB blockade at 24 or 48 hours exerts different effects on AP-1 activation and EC apoptosis is provocative and stimulating. Investigation into pathological stage- and context-dependent roles of NF-κB signaling will help to decipher the true function of NF-κB signaling in a complex pathological process.

Methods

Animal experiments. All animal experiments were approved by Institutional Animal Care and Use Committee of the Feinstein Institute for Medical Research, and performed in accordance with U.S. National Institute of Health guidelines for the care and use of laboratory animals. The creation and characterization of the EC-I-κBαmt TG mice that overexpress the I-κBαmt selectively in endothelial cells have been previously described[12]. To determine the time window minimally required for sufficient induction of I-κBαmt expression following Dox administration, TG mice were injected with Dox (0.5 mg/mouse, i.p.), and their lungs harvested 4, 6, 12 and 24 hours after Dox or 24 hours after saline injection. The tissue level of I-κBαmt mRNA was determined by qRT-PCR.

For time course studies, transgene negative littermates (WT) were injected with saline (controls) or *Escherichia coli* LPS (0111:B4, 5 mg/kg, i.p.). At 12, 18, 24, 36, 48, 96 and 144 hours following LPS injection, or 48 or 96 hours after saline injection, endothelial permeability was measured in the heart and lungs.

To examine the role of endothelial NF-κB in endothelial barrier recovery, TG mice were injected with Dox (0.5 mg/mouse, i.p.) 12, 36 or 84 hours after LPS injection to induce I-κBαmt expression and to block endothelial NF-κB at 24, 48 or 96 hours without interfering with NF-κB activity at early time points. To avoid Dox effect, WT mice were treated with Dox in the same manner. At 24, 48 or 96 hours after LPS injection, endothelial permeability was measured or organs collected for biochemical and histological analyses.

Assessment of endothelial permeability. Microvascular endothelial permeability was assessed using Evans blue dye (EBD) leakage index as a marker[42]. Mice in control and each study group were injected with EBD (20 mg/kg, i.v.) and then with heparin (200 U, i.v.) at 1.5 and 0.5 hours prior to endothelial permeability assessment. Following blood collection, organ vasculature was flushed free of blood by gentle infusion of 10 ml prewarmed PBS through left ventricle. Heart and lungs were then excised, and weighed before and after being dried at 70°C for 16 hours. Dry tissues were homogenized in formamide, incubated at 60°C for 16 hours, centrifuged, and the absorbance of the supernatant at 620 and 740 nm was recorded. Tissue intravascular residual blood contamination was corrected by subtracting A_{740} reading (tissue heme pigment content) from each A_{620} reading. Tissue EBD content (ng EBD/mg dry tissue) was calculated by comparing the corrected tissue supernatant A_{620} readings to an EBD standard curve.

To establish a causal link between the enhanced EC apoptosis and augmented endothelial permeability, additional groups of WT and TG mice were injected with caspase inhibitor, Z-VAD-FMK (3 mg/kg, i.v.) or DMSO, solvent of Z-VAD-FMK, simultaneously with LPS or saline injection, and then every 12 hours by i.p. injection. At 48 hours after LPS injection, endothelial permeability was measured.

To examine the effect of blocking the NF-κB-to-AP-1 switch at 24 hours on endothelial permeability, WT and TG mice were transfected with a pCMV-vector or pCMV-TAM67 plasmid encoding a dominant negative mutant variant of *c-Jun* (kindly provided by Dr. Tim G. Bowde, College of Pharmacy, University of Arizona, Tucson, AZ) using liposome-mediated gene transfer[23]. TAM67 lacks the major transactivation domain of *c-Jun* and blocks the function of wild type *c-Jun*[20,21]. At 3 days after transfection, mice were injected with saline, LPS and Dox, and endothelial permeability was measured at 24 hours or 48 hours after LPS injection as described above.

Analysis of EC apoptosis. In situ cell death detection kit (Roche Diagnostics, Indianapolis, IN) was used for in situ detection of apoptotic cells. Cryosections

(5 μm) were prepared from lungs of control mice or mice 24 or 48 hours after LPS challenge, fixed with paraformaldehyde, permeabilized with Triton X-100 in PBS, rinsed, and stained with Tunel reagents. Anti-CD31 (BD Bioscience, San Jose, CA) or anti-VE-cadherin antibody (Santa Cruz, Dallas, TX) was used to stain ECs followed by Alexa Fluor 594 conjugated secondary antibody (Invitrogen, Carlsbad, CA). Nuclei were counterstained with DAPI (4′, 6-diamidino-2-phenylindole). $Tunel^+$/$CD31^+$ or $Tunel^+$/$VE\text{-}cadhein^+$ apoptotic ECs in each lung cryosection was counted and expressed as a percentage of total cell nuclei.

Effect of blocking NF-κB-to-AP-1 switch on EC apoptosis. Mice in the WT-VK and TG-VK control groups were injected with PPCES vehicle (0.2 ml/mouse, i.v.) composed of 30% PEG-400, 20% polypropylene glycol, 15% Cremophor EL, 5% ethanol and 30% saline. Mice in the WT-SP and TG-SP groups were injected with a selective JNK inhibitor, SP600125 (Anthra [1, 9-cd] pyrazol-6(2H)-one, 20 mg/kg, i.v.) 15 minutes before saline or LPS (5 mg/kg, i.p.) injection. At 24 hours after LPS injection, the lungs were collected and embedded in OCT compounds for analysis of EC apoptosis. In another set of experiment, WT and TG mice were transfected with pCMV-vector or pCMV-TAM67 plasmid as described above. At 3 days after transfection, mice were injected with saline or LPS and then Dox, and euthanized 24 hours after LPS injection. Lungs were collected for analysis of EC apoptosis.

***Immunofluorescence* (IF) staining.** Tissue Bax and Bcl-2 protein expression, endothelial *c-Jun* expression and p65 nuclear translocation in lungs were analyzed by IF staining. Cryosections (3 μm) were fixed with paraformaldehyde, permeabilized with Triton X-100 in PBS, blocked with blocking reagents and stained with Bax or Bcl-2 antibody, or double stained with *c-Jun* and CD31 antibodies followed by Alexa Fluor 488 or Alexa Fluor 594 conjugated secondary antibodies as we have previously described[43].

To verify that Dox-induced I-κBαmt expression at the peak of organ injury effectively inhibits endothelial NF-κB activation *in vivo*, lung cryosections from WT and TG mice 24 hours after LPS or saline injection were stained with anti-p65 antibody followed by Alexa Fluor 488 conjugated secondary antibodies. Nuclei were counterstained with propidium iodide (PI). The number of p65 and PI double positive nuclei was used as an indicator of p65 nuclear translocation (NF-κB activation), and was compared between WT and TG mice.

Western blot. Nuclear, membrane and total proteins were extracted from cultured ECs or organs. Equal amounts of proteins were separated on 7.5–10% SDS-PAGE, and electroblotted onto nitrocellulose membrane as we previously described[12]. Immuno-localisation of specific proteins was achieved using antibodies against *c-Fos, c-Jun*, phospho-c-*Jun*, phospho-JNK, JNK, VCAM-1 and actin (Abcam, Cambridge, MA; Millipore, Billerica, MA, Santa Cruz Biotech, Dallas, TX).

***Quantitative* RT-PCR.** Total RNA was extracted using Trizol reagent (Invitrogen, Carlsbad, CA), treated with DNase I to remove traces of genomic DNA, and reverse transcribed into cDNA, which was subjected to quantitative polymerase chain reaction (qPCR) using LightCycler FastStart DNA Master SYBR Green kit as described by manufacturer (Rhoche Diagnostic, Indianapolis, IN). Q-PCR was performed in LightCycler 480 II instrument (Rhoche Diagnostic, Indianapolis, IN), using sense (5′-attatgatcctgcaagcctcgtc-3′) and antisense (5′-gcttggtcgagctgatacttccc-3′) primers. PCR product was quantified by monitoring fluorescence of DNA-binding SYBR Green dye. Plasmid containing I-κBαmt cDNA mixed with WT genomic DNA was used as template in standard curve analysis at concentrations of 1 ag to10 pg. Tissue level of Dox-induced I-κBαmt mRNA was calculated and expressed as fg cDNA in 500 ng total cDNA.

Cell culture studies. Lung microvascular ECs were isolated and cultured as we have previously described[12]. Preliminary studies were performed to titrate LPS and Dox concentrations that cause minimal *c-Jun* stimulation. ECs were left untreated, or treated with a threshold concentration of Dox (100 μg/ml). A group of untreated, or Dox treated, ECs were then stimulated with a threshold concentration of LPS (0.1 ng/ml). Cells were harvested 24 hours after Dox incubation. Nuclear protein was extracted and analyzed for nuclear levels of *c-Jun* and phospho-c-*Jun* (Ser63) proteins using Western blot or for the measurement of *c-Jun* DNA binding activity using TransAM AP-1 transcription factor assay kit (Active Motif, Carlsbad, CA).

Statistical analysis. Data were expressed as mean ± SEM and analyzed using unpaired t test or Mann-Whitney rank test for comparing two groups. For comparing multiple groups, ANOVA or Kruskal-Wallis rank test were used, followed by Holm-Sidak method or Student-Newman-Keuls Method for *post hoc* analysis. The null hypothesis was rejected at the 5% level.

1. Martin, G. S., Mannino, D. M., Eaton, S. & Moss, M. The epidemiology of sepsis in the United States from 1979 through 2000. *N Engl J Med* **348**, 1546–1554 (2003).
2. Lee, W. L. & Slutsky, A. S. Sepsis and endothelial permeability. *N. Engl. J. Med.* **363**, 689–91 (2010).
3. Aird, W. C. The role of the endothelium in severe sepsis and multiple organ dysfunction syndrome. *Blood.* **101**, 3765–77 (2003).
4. Deitch, E. A., Xu, D. & Kaise, V. L. Role of the gut in the development of injury- and shock induced SIRS and MODS: the gut-lymph hypothesis, a review. *Front Biosci.* **11**, 520–528 (2006).
5. Keel, M. & Trentz, O. Pathophysiology of polytrauma. *Injury.* **3**, 691–709 (2005).
6. Liu, S. F. & Malik, A. B. NF-κB activation as a pathologic mechanism of septic shock and inflammation. *Am. J. Physiol. Lung Cell Mol. Physiol.* **290**, L622–L645 (2006).
7. Zhao, Y. Y. *et al.* Endothelial cell-restricted disruption of FoxM1 impairs endothelial repair following LPS-induced vascular injury. *J. Clin. Invest.* **116**, 2333–43 (2006).
8. Mirza, M. K. *et al.* FoxM1 regulates re-annealing of endothelial adherens junctions through transcriptional control of beta-catenin expression. *J. Exp. Med.* **207**, 1675–85 (2010).
9. Huang, X. & Zhao, Y. Y. Transgenic expression of FoxM1 promotes endothelial repair following lung injury induced by polymicrobial sepsis in mice. *PLoS ONE* **7**, e50094 (2012).
10. Kisseleva, T. *et al.* NF-kappaB regulation of endothelial cell function during LPS-induced toxemia and cancer. *J. Clin. Invest.* **116**, 2955–2963 (2006).
11. Ashida, N. *et al.* IKKβ regulates essential functions of the vascular endothelium through kinase-dependent and -independent pathways. *Nat Commun.* **2**, 318 (2011).
12. Ye, X., Ding, J., Zhou, X., Chen, G. & Liu, S. F. Divergent roles of endothelial NF-κB in multiple organ injury and bacterial clearance in murine models of sepsis. *J. Exp. Med.* **205**, 1303–1315 (2008).
13. Bannerman, D. D. & Goldblum, S. E. Mechanisms of bacterial lipopolysaccharide-induced endothelial apoptosis. *Am. J. Physiol. Lung Cell Mol. Physiol.* **284**, L899–914 (2003).
14. Hotchkiss, R. S., Tinsley, K. W., Swanson, P. E. & Karl, I. E. Endothelial cell apoptosis in sepsis. *Crit. Care Med.* **30** (Suppl), S225–8 (2002).
15. Lin, S. J., Jan, K. M. & Chien, S. Role of dying endothelial cells in transendothelial macromolecular transport. *Arteriosclerosis* **10**, 703–709 (1990).
16. Childs, E. W., Tharakan, B., Hunter, F. A., Tinsley, J. H. & Cao, X. Apoptotic signaling induces hyperpermeability following hemorrhagic shock. *Am J Physiol Heart Circ Physiol.* **292**, H3179–89 (2007).
17. Childs, E. W. *et al.* Angiopoietin-1 inhibits intrinsic apoptotic signaling and vascular hyperpermeability following hemorrhagic shock. *Am J Physiol Heart Circ Physiol.* **294**, H2285–95 (2008).
18. Hotchkiss, R. S. *et al.* Caspase inhibitors improve survival in sepsis: a critical role of the lymphocyte. *Nat. Immunol.* **1**, 496–501 (2000).
19. Kawasaki, M. *et al.* Protection from lethal apoptosis in lipopolysaccharide-induced acute lung injury in mice by a caspase inhibitor. *Am. J. Pathol.* **157**, 597–603 (2000).
20. Brown, P. H., Chen, T. K. & Birrer, M. J. Mechanism of action of a dominant-negative mutant Of *c*-Jun. *Oncogene.* **9**, 791–9 (1994).
21. Cooper, S., Ranger-Moore, J. & Bowden, T. G. Differential inhibition of UVB-induced AP-1 and NF-kappaB transactivation by components of the jun bZIP domain. *Mol. Carcinog.* **43**, 108–16 (2005).
22. Bennett, B. L. *et al.* SP600125, an anthrapyrazolone inhibitor of Jun N-terminal kinase. *Proc. Natl. Acad. Sci. U.S.A.* **98**, 13681–13686 (2001).
23. Zhou, M. Y. *et al.* In vivo expression of neutrophil inhibitory factor via gene transfer prevents lipopolysaccharide-induced lung neutrophil infiltration and injury by a beta2 integrin-dependent mechanism. *J Clin Invest.* **101**, 2427–37 (1998).
24. Smeal, T., Binetruy, B., Mercola, D. A., Birrer, M. & Karin, M. Oncogenic and transcriptional cooperation with Ha-Ras requires phosphorylation of c-Jun on serines 63 and 73. *Nature.* **354**, 494–6 (1991).
25. Pulverer, B. J., Kyriakis, J. M., Avruch, J., Nikolakaki, E. & Woodgett, J. R. Phosphorylation of c-jun mediated by MAP kinases. *Nature.* **353**, 670–4 (1991).
26. Morton, S., Davis, R. J., McLaren, A. & Cohen, P. A reinvestigation of the multisite phosphorylation of the transcription factor c-Jun. *EMBO J.* **22**, 3876–86 (2003).
27. Ip, Y. T. & Davis, R. J. Signal transduction by the c-Jun N-terminal kinase (JNK)-from inflammation to development. *Curr Opin Cell Biol.* **10**, 205–19 (1998).
28. Mehta, D. & Malik, A. B. Signaling mechanisms regulating endothelial permeability. *Physiol Rev* **86**, 279–367 (2006).
29. Shen, Q., Rigor, R. R., Pivetti, C. D., Wu, M. H. & Yuan, S. Y. Myosin light chain kinase in microvascular endothelial barrier function. *Cardiovasc Res.* **87**, 272–280 (2010).
30. Aveleira, C. A., Lin, C. M., Abcouwer, S. F., Ambrósio, A. F. & Antonetti, D. A. TNF-α signals through PKCζ/NF-κB to alter the tight junction complex and increase retinal endothelial cell permeability. *Diabetes.* **59**, 2872–82 (2010).
31. He, F. *et al.* RhoA and NF-κB are involved in lipopolysaccharide-induced brain microvascular cell line hyperpermeability. *Neuroscience.* **188**, 35–47 (2011).
32. Kyritsis, N. *et al.* Acute inflammation initiates the regenerative response in the adult zebrafish brain. *Science* **338**, 1353–1356 (2012).
33. Tang, G. *et al.* Inhibition of JNK activation through NF-kappaB target genes. *Nature.* **414**, 313–7 (2001).
34. Reuther-Madrid, J. Y. *et al.* The p65/RelA subunit of NF-kappaB suppresses the sustained, antiapoptotic activity of Jun kinase induced by tumor necrosis factor. *Mol Cell Biol.* **22**, 8175–3 (2002).
35. Papa, S. *et al.* Gadd45 beta mediates the NF-kappa B suppression of JNK signalling by targeting MKK7/JNKK2. *Nat Cell Biol.* **6**, 146–53 (2004).
36. Rahman, A. & Fazal, F. Blocking NF-κB: an inflammatory issue. *Proc Am Thorac Soc.* **8**, 497–503 (2011).
37. Pasparakis, M. Regulation of tissue homeostasis by NF-kappaB signalling: implications for inflammatory diseases. *Nat Rev Immunol* **9**, 778–88 (2009).

38. Fong, C. H. *et al*. An antiinflammatory role for IKKbeta through the inhibition of "classical" macrophage activation. *J Exp Med.* **205**, 1269–76 (2008).
39. Chiang, S. H. *et al*. The protein kinase IKKepsilon regulates energy balance in obese mice. *Cell.* **138**, 961–75 (2009).
40. Greten, F. R. *et al*. NF-kappaB is a negative regulator of IL-1beta secretion as revealed by genetic and pharmacological inhibition of IKKbeta. *Cell.* **130**, 918–31 (2007).
41. Arkan, M. C. *et al*. IKK-beta links inflammation to obesity-induced insulin resistance. *Nat Med.* **11**, 191–8 (2005).
42. Wang, l. F. *et al*. Role of inducible nitric oxide synthase in pulmonary microvascular protein leak in murine sepsis. *Am J Respir Crit Care Med.* **165**, 1634–1639 (2002).
43. Song, D., Ye, X., Xu, H. & Liu, S. F. Activation of endothelial intrinsic NF-κB pathway impairs. *Blood.* **114**, 2521–2529 (2009).

Acknowledgments

We thank Dr. Tim Bowde, University of Arizona, for providing the pCMV-TAM67 plasmid, and Dr. Dongmei Song for technical advice on immunofluorescence staining. This work was supported by NIH grants AI076987(SFL) and AHA grant 12GRNT1214002 (SFL).

Author contributions

S.F.L. proposed the hypothesis, designed the experiments and wrote the manuscript. G.L. and X.Y. performed the experiments and data analyses. E.J.M. significantly edited the manuscript.

Additional information

Ethics statement The methods were carried out in accordance with U.S. National Institute of Health guidelines for the care and use of laboratory animals.

Supplementary information accompanies this paper at http://www.nature.com/scientificreports

Competing financial interests: The authors declare no competing financial interests.

How to cite this article: Liu, G., Ye, X.B., Miller, E.J. & Liu, S.F. NF-κB-to-AP-1 Switch: A Mechanism Regulating Transition From Endothelial Barrier Injury to Repair in Endotoxemic Mice. *Sci. Rep.* **4**, 5543; DOI:10.1038/srep05543 (2014).